Charging of large dust grains in flowing plasmas

N. Rizopoulou,[1,*] A. P. L. Robinson,[2] M. Coppins,[1] and M. Bacharis[1]
[1]*Blackett Laboratory, Imperial College London, Prince Consort Road, London SW7 2BZ, United Kingdom*
[2]*Central Laser Facility, Rutherford-Appleton Laboratory, Chilton, Oxon OX11 0QX, United Kingdom*
(Received 21 November 2014; published 10 June 2015)

The charging of a large dust grain immersed in a flowing plasma is important for the study of several phenomena and in many applications. It is shown that in order to understand the charging mechanism of large dust grains, it is of great importance to take into account and calculate the effect of plasma flows on the sheath that develops around them.

DOI: 10.1103/PhysRevE.91.063103 PACS number(s): 52.27.Lw, 52.40.Kh, 52.55.Rk, 94.05.Jq

I. INTRODUCTION

The problem of the charging of an object immersed in a flowing plasma is important for the study of several phenomena in space, atmospheric, and laboratory plasmas [1]. Such objects come in a variety of sizes; however, the important factor for determining the physics of their charging is not their absolute size but how this compares with the electron Debye length; when their size is larger than this characteristic length, we refer to them as large dust grains. Four examples of systems where the role of large dust grains immersed in a flowing plasma is important include objects in the solar system, like comets in large heliocentric distances [1–4], the Moon [5,6], the charging of spacecraft [7–11], and the theoretical modeling of dust transport in magnetic fusion reactors [12–17]. In all these cases understanding the charging process is central for understanding the dynamics of these systems. The same physics is also important for understanding plasma diagnostics and in particular, probe theory and the measurement of plasma flows [18–23].

A consistent theory that calculates the charging of large dust grains is important. The orbital motion limited (OML) approach [24,25] is the most widely used theory for determining the charge of a dust grain in a plasma, but although it gives good results for small dust grains, for large dust grains is inadequate [26,27]. Other more accurate approaches do not address the effect of flows [26]. An effort to address these limitations was also presented in the literature in the form of the modified orbital motion limited (MOML) theory [28]. However, MOML fails to recover and explain important characteristics of such systems [28].

In this article, we introduce the insight that modifications of the sheath's characteristics due to plasma flows can affect the physics of the dust-plasma interaction. We study how this affects the charging mechanism, a crucial parameter for the dynamics of dust grains immersed in plasmas. Furthermore, we present a theoretical model for the charging of large dust grains in flowing plasmas that can take this effect into account. We call this model MOML-FL.

II. THE MOML-FL THEORY

The MOML theory, as it was presented in [28], attempts to give an answer to the question of what is the floating potential of dust grains which are much larger than the electron Debye length, where λ_{De} is a characteristic plasma length scale given by $\lambda_{De} = (k_B T_e/4\pi n_e e^2)^{1/2}$, where k_B is the Boltzmann constant, T_e the electron plasma temperature, n_e is the electron plasma number density, and e is the electron charge. In this case, the dust grain develops a sheath around its surface; the dimensions of the sheath are of the order of the electron Debye length, so its width is much smaller than the radius of the dust grain. As there is now a clearly developed sheath around the particle, its characteristic properties can be used for the calculation of the grain's potential. In particular, the potential drop in the sheath from the planar case can be calculated. In principle, OML can be applied for any surface as long as a link can be established between the potential of this surface and the potential of the dust grain. This link exists for the sheath's edge. Based on this, in MOML, the calculation of the ion current can be split into two stages. In the first stage, OML can be applied in order to find the ion current to the edge of the developed sheath. The advantage of this approach is that the majority of the absorption radii are located within the sheath region, and therefore the effect of absorption radii in the region where the ion current is calculated through OML is negligible [28]. The second stage is to link the potential at the sheath's edge with the potential of the grain's surface. This is done by calculating the potential drop across the sheath. In MOML, the potential drop from the sheath's edge to the surface is calculated using the thin sheath approximation [28].

For the cases that τ is larger than 1, where τ is the ratio of the ion to the electron temperature, the agreement between MOML and the results of the particle-in-cell (PIC) simulation code SCEPTIC [29–33] is good (see Figs. 6 and 7). However, for values smaller than 1 there are two problems. The first is that the agreement between MOML and SCEPTIC results for cases $\tau = 0.1$ and $\tau = 0.01$ is not as good as in the case with $\tau = 1$ and $\tau = 10$. The second problem is that MOML seems to miss important characteristics of the behavior that are being exhibited in the simulated results from SCEPTIC. This is mainly observed in a window approximately between 0.5 and 1.5 v_{BC}; $v_{BC} = \sqrt{\frac{kT_e}{M}}$ is the Bohm velocity for cold ions, where T_e is the electron temperature and M is the ion mass.

In [28,30] these features have been attributed to the transition between a regime where dust grain charging is dominated by electrostatic and thermal effects (relevant for stationary and slow flowing plasmas) and a regime where dust grain charging is dominated by plasma flows. This

*nikoleta.rizopoulou06@imperial.ac.uk

transition, as argued in [28,30], is smooth for $\tau \geqslant 0.5$ but it is very sudden in cases where the value of τ is smaller. This phenomenon, according to [28], explains the discrepancies between MOML and SCEPTIC results for the cases of $\tau = 0.1$ and $\tau = 0.01$. Additionally, for $\tau = 0.01$ a second reason for these discrepancies cited again in [28] is the fact that SCEPTIC is affected by numerical heating for very low ion temperatures.

In Fig. 4 in Willis *et al.* 2012 [28], the potential distribution around the dust grain for three different plasma flows v/v_{BC}= 0.3, 0.9, 1.3 and for $\tau = 0.2$ was presented. It can be observed that the potential distribution in the upstream side of the grain is also affected by increasing the plasma flow velocity. More specifically, the spatial dimensions of the sheath's structure in front of the particle decrease, while the plasma flow velocity increases. Such compression of the spatial dimensions of the planar sheath in a source-collector sheath system as a function of the flow velocity was observed in [34]. This was also coupled with differences in the observed potential drop in the sheath compared with the no-flow case (see Fig. 3).

Here we present the MOML-FL theory that calculates the potential of a large dust grain in a flowing plasma taking into account the effect of flows in the plasma sheath. In the MOML-FL, instead of using a potential drop that is independent of the flow velocity like in the MOML theory, we use the results of [34] where the calculated potential drop in the sheath is a function of the flow velocity.

The results in [34] were calculated for the source-collector sheath system where shifted Maxwellian distributions were used in the source boundary. In this case there was the development of both a source and a collector sheath. In MOML-FL, we use the normalized potential difference between the wall (collector) ψ_c and the edge of the source sheath ψ_s. This is given by $\Delta\psi = \psi_c - \psi_s$, which is the potential drop across the collector sheath (see Fig. 1). The values of ψ_c and ψ_s were calculated in [34] using current balance at the wall (collector) and the quasineutrality condition between the end of the source sheath and the start of the collector sheath. In Fig. 2 we plot the potential drop of the normalized potential $\Delta\psi$ from the MOML and from the source-collector sheath's theoretical model for a stationary plasma. Comparing the two,

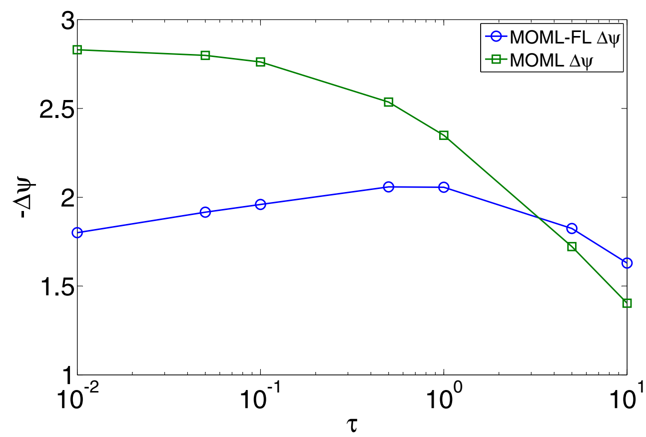

FIG. 2. (Color online) The normalized potential drop $\Delta\psi$ as a function of τ. This is calculated as in Willis *et al.* [28], denoted as MOML, and in MOML-FL for $v = 0$, for hydrogen.

it can be seen that value of the $\Delta\psi$ assumed in MOML is significantly larger than the one used in MOML-FL for small values of τ. This is because the two models are based on different assumptions. For example, the sheath model assumes the Bohm velocity v_B at the sheath's edge, whereas, in the source-collector sheath system the Bohm criterion is oversatisfied (see [34]) and $v > v_B$ at the edge of the collector sheath. More specifically, the percentage difference between the two is approximately 57% for $\tau = 0.01$. As the value of τ increases, the difference between the two values decreases, and for $\tau = 10$ the value of the $\Delta\psi$ calculated from the source-collector sheath theoretical model is larger than the one assumed in MOML, with a percentage difference of the order of 14%.

For this reason, we examine two different cases in MOML-FL: one with constant $\Delta\psi$, calculated for $v = 0$, similar to the case of MOML (see Fig. 2), and in the other we use a $\Delta\psi$ that it is a function of the plasma flow velocity (see Fig. 3).

We can now calculate the MOML-FL floating potential by implementing the flow-dependent $\Delta\psi$ in the MOML current

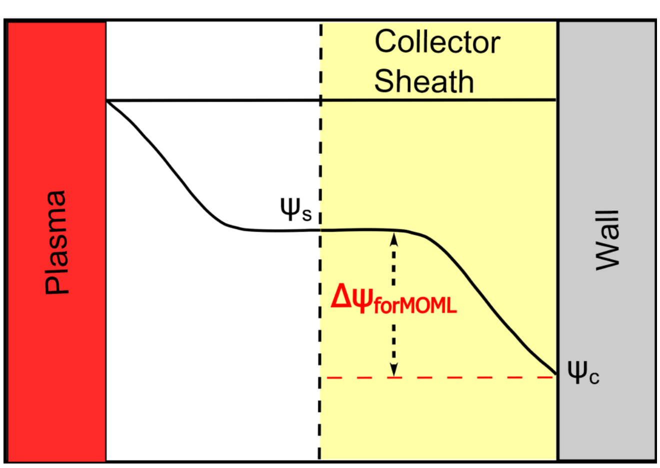

FIG. 1. (Color online) A graphic representation of the potential drop from the source-collector sheath theoretical model that was used to replace the sheath potential drop in the MOML-FL theory.

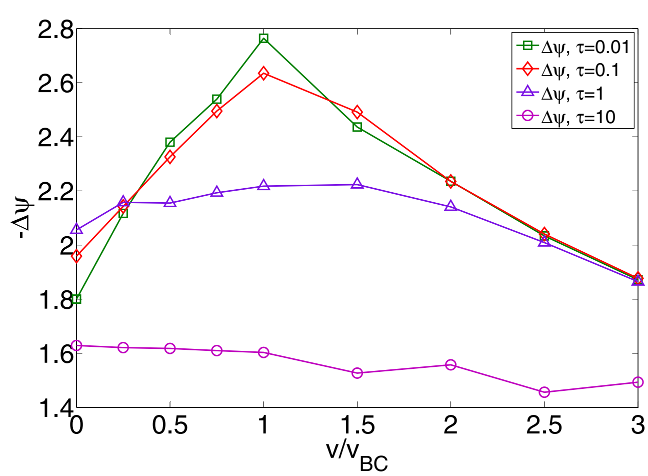

FIG. 3. (Color online) The normalized potential drop calculated by the source-collector sheath's theoretical model as a function of the normalized velocity for cases $\tau = 0.01$, 0.1, 1, and 10, for hydrogen.

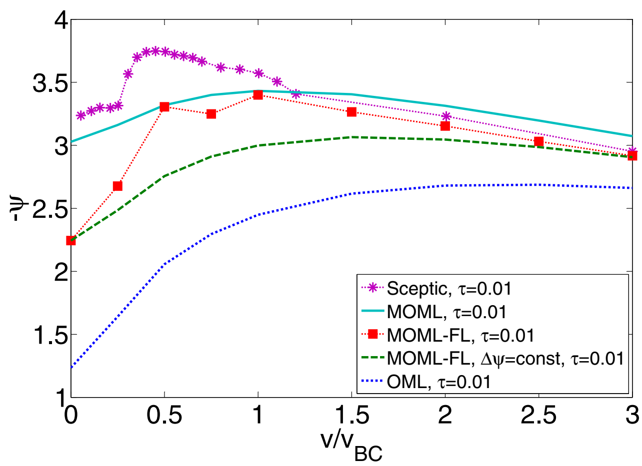

FIG. 4. (Color online) The negative normalized floating potential with respect to the normalized velocity for the case $\tau = 0.01$ for five different cases, for hydrogen.

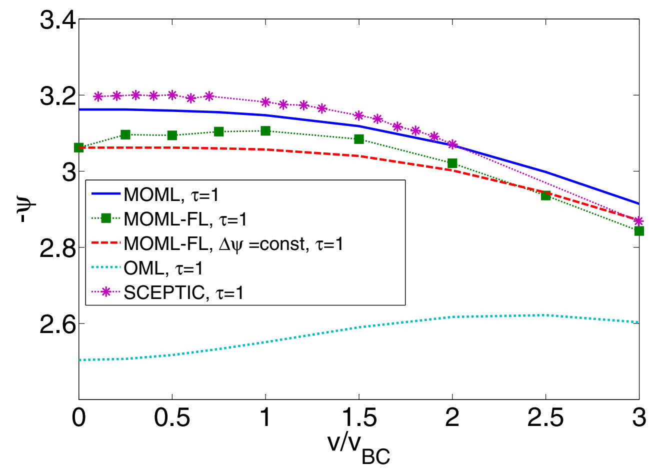

FIG. 6. (Color online) The negative normalized floating potential with respect to normalized velocity for the case $\tau = 1$ for five different cases, for hydrogen.

balance,

$$\exp(\psi) = \sqrt{\tau\mu}\left[F_1\left(\frac{u}{\sqrt{2\tau}}\right) - F_2\left(\frac{u}{\sqrt{2\tau}}\right)\frac{\psi - \Delta\psi}{\tau}\right], \quad (1)$$

where ψ is the floating potential normalized with respect to the electron temperature, τ is the ratio of the ion-to-electron temperature, μ is the ratio of the electron-to-ion mass, u is the plasma flow velocity normalized with respect to the Bohm velocity for cold ions, and F_1 and F_2 are given in the equations below:

$$F_1(\chi) = \frac{1}{4}\sqrt{\pi}(1 + 2\chi^2)\frac{\text{erf}(\chi)}{\chi} + \frac{1}{2}\exp(-\chi^2), \quad (2)$$

$$F_2(\chi) = \frac{1}{2}\sqrt{\pi}\frac{\text{erf}(\chi)}{\chi}. \quad (3)$$

The results of the above calculation can be seen in Figs. 4–7. Comparing our results for constant $\Delta\psi$ (which is what MOML does) with our results where $\Delta\psi$ changes with flow velocity, we observe that the lost SCEPTIC features in MOML for cases of $\tau = 0.01, 0.1, 1$ in Ref. [28] are being recovered when taking into account the effect of the plasma flow velocity to the sheath's structure, i.e., when $\Delta\psi$ changes also with flow velocity. In particular, the steep increase observed in the SCEPTIC results for low ion temperatures ($\tau = 0.01$ and 0.1) and for velocities between $0.5v_{BC}$ and $1.5v_{BC}$ is recovered in MOML-FL when taking into account the effect of flows to the plasma sheath.

Furthermore, by directly examining the percentage difference between the MOML approach and the SCEPTIC results and the corresponding difference for the MOML-FL we observe the following. In general, the agreement with the SCEPTIC results becomes better for higher values of τ and higher normalized velocities for both the MOML and the MOML-FL, for example, the difference between the SCEPTIC results and MOML ranges from approximately 30% for $\tau = 0.01$ for the stationary case to approximately 0.5% for $\tau = 10$, whereas for the MOML-FL this difference ranges from 25% for the stationary case with $\tau = 0.01$ to 0.6% for $\tau = 10$.

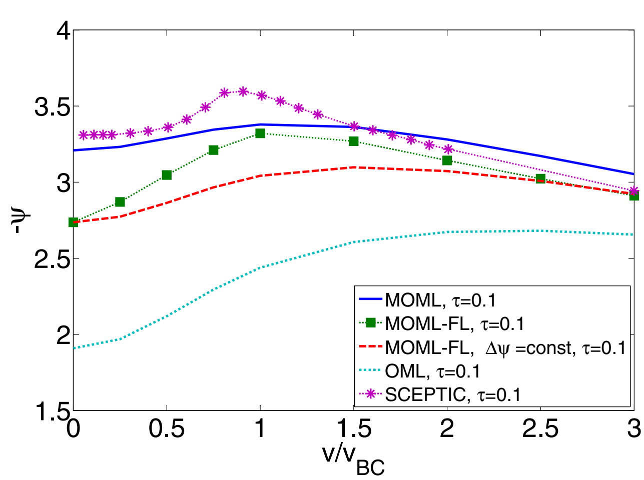

FIG. 5. (Color online) The negative normalized floating potential with respect to normalized velocity for the case $\tau = 0.1$ for five different cases, for hydrogen.

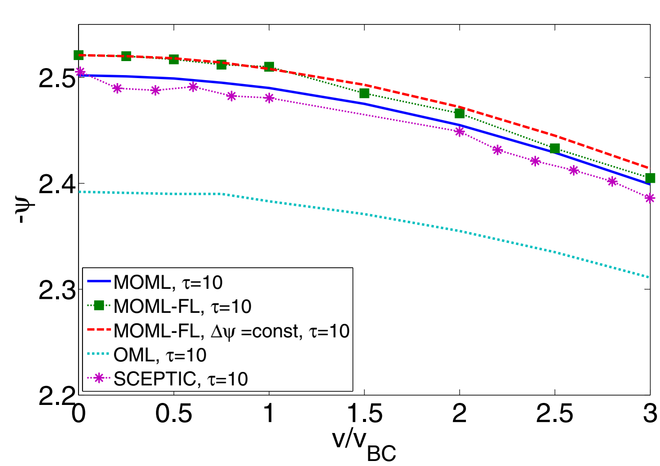

FIG. 7. (Color online) The negative normalized floating potential with respect to normalized velocity for the case $\tau = 10$ for five different cases, for hydrogen.

For low normalized velocities up to v_{BC}, we can observe that the agreement of the MOML results is better compared to MOML-FL. However, this changes for normalized velocities greater than v_{BC}, where the agreement of the two approaches with SCEPTIC becomes comparable and even in some cases the MOML-FL model has a better agreement with the SCEPTIC results than MOML. For example, for normalized velocity $1.5v_{BC}$ and $\tau = 0.01$ and the difference of the MOML result with SCEPTIC is of the order of 5%, whereas for the MOML-FL model this difference is of the order of 0.6%. This is because at high velocities where the effect of flow is dominant, our approach describes not only the effect of flows in the charging cross section but also its effect to the grain's sheath.

Also, the agreement between MOML-FL and SCEPTIC improves for higher velocities for the cases with $\tau = 0.01, 0.1, 1$, where, for example, the difference between the MOML-FL model and SCEPTIC results for $\tau = 0.1$ varies from around 18% in the stationary case to around 1% for a normalized velocity of $3v_{BC}$.

III. CONCLUSIONS

In conclusion, we have introduced the effect of flows to the sheath in the description of the physics of the dust-plasma interaction. The resulting theory (MOML-FL) recovers previously unexplained features found in numerical simulations examining the charging of large dust grains. The potential impact of our finding spans a wide region of physics where plasma-dust interactions are involved, such as space physics, astrophysics, magnetic confinement fusion, plasma processing, and plasma diagnostics.

ACKNOWLEDGMENTS

The authors are grateful for the use of Yggdrasil provided by STFC's Central Laser Facility. N.R. would like to thank Dr. Claudio Bellei, Dr. Chris Willis, and Prof. John Allen for useful discussions. This work was financially supported by the UK Engineering and Physical Sciences Research Council (EPSRC).

[1] P. K. Shukla and A. A. Mamun, *Introduction to Dusty Plasma Physics* (Institute of Physics Publishing, Ltd., Bristol, UK, 2002).
[2] D. A. Mendis and M. Horányi, Rev. Geophys. **51**, 53 (2013).
[3] A. J. Coates, Adv. Space Res. **33**, 1977 (2004).
[4] D. A. Mendis, J. R. Hill, H. L. Houpis, and E. C. Whipple, Astrophys. J. **249**, 787 (1981).
[5] J. S. Halekas, Y. Saito, G. T. Delory, and W. M. Farrell, Planet. Space Sci. **59**, 1681 (2011).
[6] T. Nitter and O. Havnes, Earth, Moon, Planets **56**, 7 (1992).
[7] A. Sjogren, A. I. Eriksson, and C. M. Cully, IEEE Trans. Plasma Sci. **40**, 1257 (2012).
[8] J. Olson, W. J. Miloch, S. Ratynskaia, and V. Yaroshenko, Phys. Plasmas **17**, 102904 (2010).
[9] H.-W. Hsu, M. Horányi, S. Kempf, and E. Grün, Geophys. Res. Lett. **39**, 6 (2012).
[10] V. V. Yaroshenko, W. J. Miloch, H. M. Thomas, and G. E. Morfill, Geophys. Res. Lett. **39**, 18 (2012).
[11] V. V. Yaroshenko, W. J. Miloch, S. Vladimirov, H. M. Thomas, and G. E. Morfill, J. Geophys. Res.: Space Phys. (1978-2012) **116**, A12 (2011).
[12] M. Sertoli, J. C. Flanagan, M. Bacharis, O. Kardaun, A. Jarvinen, G. F. Matthews, S. Brezinsek, D. Harting, A. Cackett, E. Hodille, I. H. Coffey, E. Lazzaro, and T. Pütterich, JET-EFDA Contributors J. Nucl. Mater. (2014).
[13] J. C. Flanagan, M. Sertoli, M. Bacharis, G. F. Matthews, P. de Vries, A. Widdowson, I. H. Coffey, G. Arnoux, B. Sieglin, S. Brezinsek *et al.*, Plasma Phys. Controlled Fusion **57**, 014037 (2015).
[14] J. Winter, Plasma Phys. Controlled Fusion **40**, 1201 (1998).
[15] G. De Temmerman, M. Bacharis, J. Dowling, and S. Lisgo, Nucl. Fusion **50**, 105012 (2010).
[16] R. D. Smirnov, A. Yu Pigarov, M. Rosenberg, S. I. Krasheninnikov, and D. A. Mendis, Plasma Phys. Controlled Fusion **49**, 347 (2007).
[17] M. Bacharis, M. Coppins, and J. E. Allen, Phys. Plasmas (1994-present) **17**, 042505 (2010).
[18] M. Hudis and L. M. Lidsky, J. Appl. Phys. **41**, 5011 (1970).
[19] I. H. Hutchinson, Phys. Plasmas **9**, 1832 (2002).
[20] L. Oksuz and N. Hershkowitz, Plasma Sources Sci. Technol. **13**, 263 (2004).
[21] L. Patacchini and I. H. Hutchinson, Phys. Rev. E **80**, 036403 (2009).
[22] I. H. Hutchinson and L. Patacchini, Plasma Phys. Controlled Fusion **52**, 124005 (2010).
[23] L. Patacchini and I. H. Hutchinson, Plasma Phys. Controlled Fusion **52**, 035005 (2010).
[24] H. Mott-Smith and I. Langmuir, Phys. Rev. **28**, 727 (1926).
[25] J. E. Allen, Phys. Scr. **45**, 497 (1992).
[26] R. V. Kennedy and J. E. Allen, J. Plasma Phys. **69**, 485 (2003).
[27] J. E. Allen, B. M. Annaratone, and U. de Angelis, J. Plasma Phys. **63**, 299 (2000).
[28] C. T. N. Willis, M. Coppins, M. Bacharis, and J. E. Allen, Phys. Rev. E **85**, 036403 (2012).
[29] I. H. Hutchinson, Plasma Phys. Controlled Fusion **44**, 1953 (2002).
[30] I. H. Hutchinson, Plasma Phys. Controlled Fusion **45**, 1477 (2003).
[31] L. Patacchini and I. H. Hutchinson, Plasma Phys. Controlled Fusion **49**, 1719 (2007).
[32] L. Patacchini and I. H. Hutchinson, Plasma Phys. Controlled Fusion **49**, 1193 (2007).
[33] I. H. Hutchinson and L Patacchini, Phys. Plasmas **14**, 013505 (2007).
[34] N. Rizopoulou, A. P. L. Robinson, M. Coppins, and M. Bacharis, Plasma Sources Sci. Technol. **22**, 035003 (2013).